Original Paper

Strength optimization of glass containers by the finite element method

Hayo Müller-Simon und Hansjürgen Barklage-Hilgefort
Hüttentechnische Vereinigung der Deutschen Glasindustrie (HVG), Frankfurt am Main (FRG)

A finite element program to calculate the wall stresses of container glass with respect to axial loads and internal pressure loads has been installed in a microcomputer. The stress calculations are based on a modified shell element. The efficiency of this element type as well as the working properties of the finite element program were tested. Sample bottles and the corresponding bursting pressure data were available for this investigation. From these data, maximum permissible wall stresses were calculated with the finite element program. The results were found to be in the same range as those stated in the literature. The finite element program gives a fast and sufficiently accurate prediction of the influence of changes in glass container outline or glass distribution by calculation.

Festigkeitsoptimierung von Hohlglasbehältern durch die Finite-Elemente-Methode

Ein Finite-Elemente-Programm für die Berechnung von Wandspannungen an Hohlglasbehältern unter Innendruck oder axialer Belastung wurde auf einem Mikrocomputer installiert. Den Spannungsberechnungen liegt ein modifiziertes Schalenelement zugrunde. Die Leistungsfähigkeit des Elementtyps und die Betriebseigenschaften des Programms wurden getestet. Für die Untersuchungen standen Probeflaschen und die zugehörigen Berstdruckdaten zur Verfügung. Hieraus wurden mit dem Programm maximal zulässige Wandspannungen berechnet. Die Ergebnisse stimmen größenordnungsmäßig mit den Angaben in der Literatur überein. Das Finite-Elemente-Programm erlaubt eine schnelle und ausreichend genaue Berechnung der Wandspannungen, um den Einfluß von Änderungen der Kontur oder der Glasverteilung vorherzusagen.

1. Introduction

When planning and designing glass containers many different influencing factors have to be born in mind. The glass must suit the molding conditions in the container glass machine; the containers must satisfy the requirements of the filling line and of the capping machines; they must be consumer friendly and have a good standing stability. Especially when filled with carbonated drinks the bottles must have a sufficiently high internal pressure strength. The axial load strength must be such that in the capping machine and during stacking no breakage occurs. The weight of the container must be low so as to economize the costs of raw materials and energy and so as to ease transport. Besides this, the container must have an attractive design and must require little storage place.

Most of these demands are associated with the container strength. In order to obtain strength information in the past, one had to rely on experiments, because strength calculation is impossible by classical methods. However, experimental strength values vary over a broad range on account of the special properties of the material glass.

Received 31 August 1988.
Eine ausführlichere Fassung dieser Arbeit in deutscher Sprache liegt in der Bibliothek der Deutschen Glastechnischen Gesellschaft, Mendelssohnstraße 75–77, D-6000 Frankfurt 1, vor.

During the past few years developments in semiconductor electronics have led to the production of more efficient microcomputers at falling prices. The result has been a rapid evolution of numerical methods for strength calculations. The finite element method has especially opened up the possibility of carrying out more container glass calculations.

The present investigation is concerned with the possibilities which the use of finite element calculations will offer to the design engineer, even using a microcomputer with limited storage capacity, for testing rapidly and sufficiently accurate the local stresses caused by internal pressure or axial load in a specific container design.

1.1. Strength of glass and mechanical fracture considerations

The theoretical strength of glass is very high with a maximum tensile stress of about $\sigma_B \approx 10^4$ MPa. However, in practice only a fracture stress of about 100 MPa is achieved. This clear difference is caused by the strong influence of the state of the glass surface on the strength. In the course of production, glass containers have repeated contact with other bodies, so that the surface becomes more or less damaged and a large number of small flaws are formed. Fracture mechanics show that at the crack tip stresses can easily arise which lie in the order of magnitude of the theoretical strength. While such stresses can be dissipated in ductile materials, such as metals, by plastic deformation in the microscopic range, in brittle materials they lead to fracture.

A theoretical description of the strength properties of glass is given by linear elastic fracture mechanics. For this purpose, the mechanical behavior of a single flaw in a linear-elastic, homogeneous and isotropic continuum is considered. The strain which leads to failure can be traced back to three fundamental types of stress: stress perpendicular to the flaw's orientation (mode I), shearing stress perpendicular to the specimen's surface (mode II) and shearing stress parallel to the flaw (mode III).

In order to make some statement about the failure of a glass object, fracture mechanics examine the most expandable crack. For a surface crack with the depth a the danger of fracture under mode I strain is characterized by the stress intensity factor

$$K_{\mathrm{I}} = \sigma_0 \sqrt{a}\, f\,(\text{geometry})\;, \tag{1}$$

where σ_0 is the stress applied to the glass object and f is a correction function depending on the flaw and specimen geometry. In the case of brittle crack propagation the stress intensity factor of mode I strain K_{I} is an important quantity. The crack propagation velocity v_{c} depends on K_{I} and possible environment-dependent parameters P_{E}, which consider humidity and temperature:

$$v_{\mathrm{c}} = f\,(K_{\mathrm{I}}, P_{\mathrm{E}})\;. \tag{2}$$

If

$$\mathrm{d}v_{\mathrm{c}}/\mathrm{d}a > 0\;, \tag{3}$$

the crack becomes instable and the specimen fails. In this case K_{I} reaches a for the given environment critical value K_{Ic} [1].

The strength of a glass container is already critically lowered by microscopically small flaws. The size of these flaws is small compared with the surface curvature of the container in the neighborhood of the flaw. Thus, the influence of the specimen geometry is taken into consideration by the local dependence of the applied surface stress.

A detailed investigation of the influence of surface damage on the strength of glass rods has been carried out by Varner and Oel [2]. For this investigation Sommer [3] shows that a correlation between experimental results and fracture mechanics can be found by deducing critical stress intensity factors for different crack models. If the stress distribution along a container contour is calculated by a finite element program, it should be possible to estimate the container strength from the probability of damages to appear and from the type of damage involved.

2. Stress calculation by the finite element method

The finite element method enables the calculation of stress distributions in complex bodies, even when a consistent solution is not known. For this purpose the problem is split up into discrete points, i.e. the object is described by a network of elements, in which the stress is only calculated by a finite number of nodes.

The procedure of working with finite element programs can be split up into the following steps:

a) The container shape data are read into the computer.

b) The shape is subdivided into discrete pieces of suitable form and size.

c) The stiffness matrix and the applied load vector are built up by the element matrices and element vectors of a chosen element type, which describe the elastic properties of the element. With a clever element arrangement the stiffness matrix can be made having a slightly occupied band structure. This enables a very economical use of the computer storage capacity.

d) The stiffness matrix and the applied load vector have to be modified according to the environmental conditions. In this step the support point as well as the load are taken into account.

e) The resulting system of linear equations now has to be solved. This part of the calculation is done by special subprograms, which are optimized especially with respect to the time requirements.

f) The calculated wall stress distribution is printed.

For carrying out the stress calculations in the course of this investigation, a finite element program was used which was developed at the "Institut für Technische Mechanik, RWTH Aachen" on behalf of the HVG [4]. The program was installed on a DEC-LSI-11 with a 64 kbyte memory.

2.1. Selection of the element type

The choice of the element type is of great importance for the power of a finite element program. A criterion which primarily reduces the facilities of the element choice is the limitation of computer storage capacity. For this reason, three-dimensional elements have to be excluded. As a first approximation in the case of container glass rotational elements are suitable. However, this simplification is not sufficient to realize a finite element program at the microcomputer in use. A further approximation is the installation of a plate or shell model to describe the glass container. For that purpose, the wall thickness w is assumed to be small compared with the container's measurements, especially the radius of curvature R. In this case the mechanical quantities can be projected on the mean plane of the container wall as a good

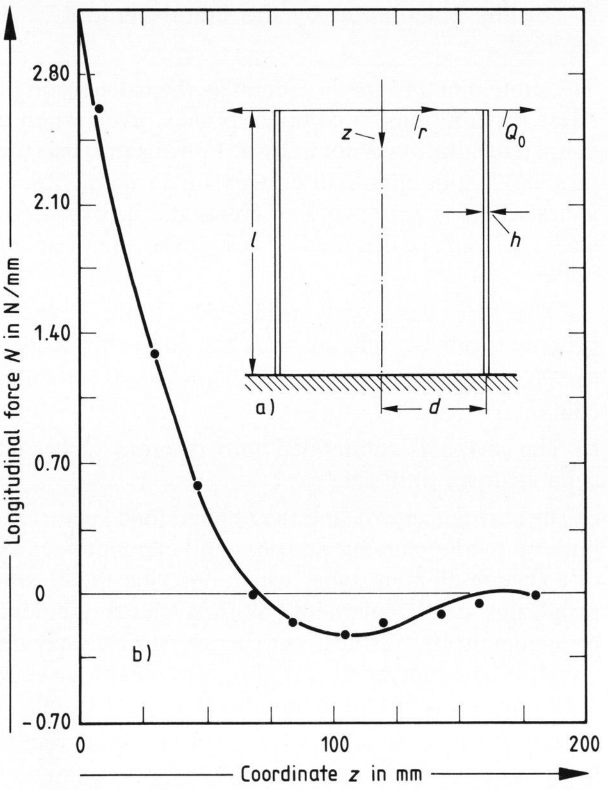

Figures 1a and b. Calculation of the longitudinal force N on a thin wall tube under transverse load Q_0 at the end; a) schematic longitudinal section of the thin wall tube, b) longitudinal force N calculated by the finite element program (●) in comparison to its representation in curve (———) according to [5]. Following parameters are inserted for the calculation: modulus of elasticity $E = 6.9 \cdot 10^5$ MPa, Poisson's number $\nu = 0.3$, tube radius $d = 127$ mm, length $l = 152.4$ mm, wall thickness $h = 0.254$ mm, transverse load $Q_0 = 44.5$ N.

approximation, so that it is now possible to reduce the problem by another dimension. With such an element type fairly fast finite element programs can be set up on microcomputers.

However, in the bottom region of a bottle the assumption that the wall thickness w is much smaller than the radius R is not accurate. Moreover bottles are especially endangered to fracture in this region, so deviations in the calculation are very unsatisfactory. This is the reason for the development of a shell element which considers shear deformation, as to be expected in the case of thick shells, and which furthermore considers first order of (w/R) terms [4]. In fact the new shell element needs more computer storage space, but leads to much better results, so that the additional requirement for storage can be justified.

Furthermore, the description of the outline should be as simple as possible. The shape of glass containers suggests a choice of spherical and cylindrical elements. A restriction on cylindrical shells, i.e. straight connections between the points of a rotational object, would require too many elements in the case of a small radius of curvature to get a sufficient resolution of the shape. Hence the installed finite element program uses spherical and cylindrical shells.

2.2. Estimation of the results with the chosen element type

In order to test the used shell element in [4], a few examples have been calculated, for which consistent or approximated solutions are known. Figure 1a shows the example of a thin wall tube under lateral strain at one end, figure 1b shows the forces in the circumferential direction. The points in figure 1b are the values obtained by finite element calculation, which shows a very good fit. The second example is a sphere segment under uniform surface load P, as shown in figure 2a. The comparison with an approximation regarding the bending moment and the longitudinal force, as given by [5], are shown in figures 2b and c. Again, in this example, both calculations fit well.

Test calculations carried out by Kopetsch [4] were based on problems of thin shells with $w \ll R$. However, this assumption does not hold for every region of a glass container, especially the bottom. Although there are no comparable calculations between the chosen element type and some possible continuum model-based calculations, some details will be given which enable an estimation of the calculated stress values of actual glass bottles.

3. Working with the finite element program

3.1. Handling of the outline data

In the glass industry it is common to describe a glass container outline with circles and straight lines. Because this method of description is the foundation of all structural data, it leads itself as a base for the input to the relevant finite element program. The shape of the glass container is described in segments by the specification of the radius of curvature, at the starting and finishing point of the segment, as taken from structural data, also by the wall thickness both at the starting and the finishing point, as found on sample bottles. This method of description has the advantage that the entire outline can be determined by a minimum of data.

The first version of the finite element program checked the outer surface of bends. However, if in a region considerable variations of the wall thickness appear, in the case of an outer surface without a bend, by necessity bends result in the mean plane which leads to wrong stress values at that point. Moreover, it appears that, especially in the bottom region, it is often impossible to generate an outline of circles which sufficiently approximates the sample bottle with its glass distribution. For this reason the mode of input was changed. Instead of the outer

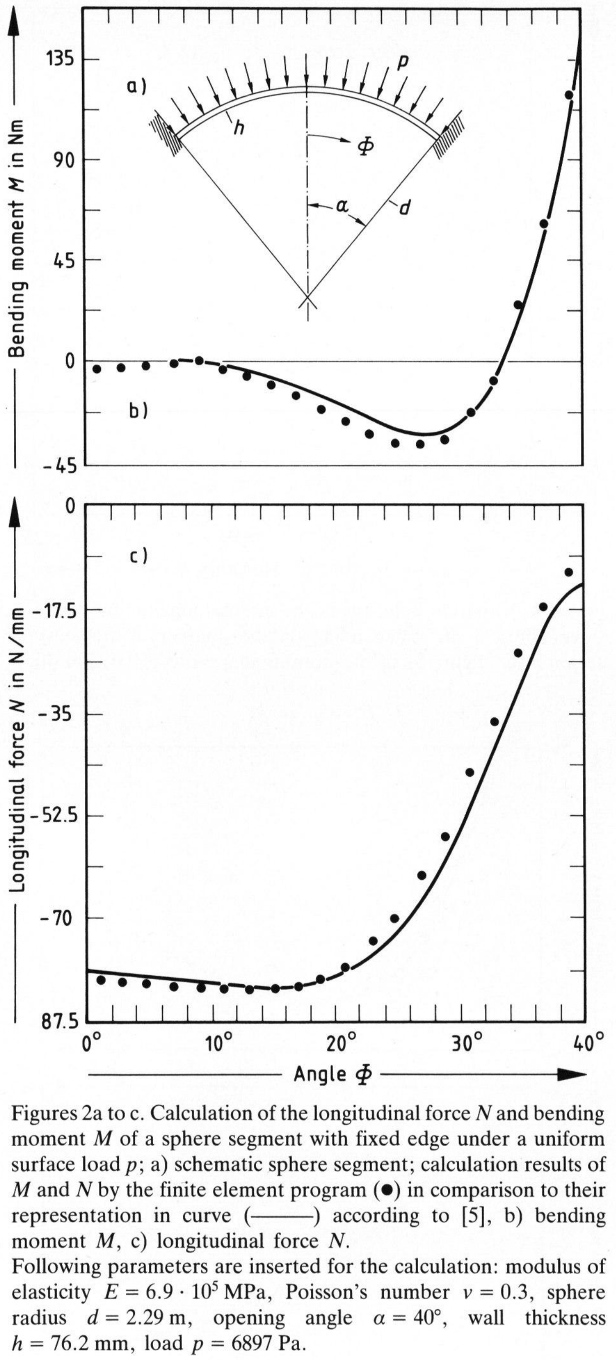

Figures 2a to c. Calculation of the longitudinal force *N* and bending moment *M* of a sphere segment with fixed edge under a uniform surface load *p*; a) schematic sphere segment; calculation results of *M* and *N* by the finite element program (●) in comparison to their representation in curve (———) according to [5], b) bending moment *M*, c) longitudinal force *N*.
Following parameters are inserted for the calculation: modulus of elasticity $E = 6.9 \cdot 10^5$ MPa, Poisson's number $\nu = 0.3$, sphere radius $d = 2.29$ m, opening angle $\alpha = 40°$, wall thickness $h = 76.2$ mm, load $p = 6897$ Pa.

surface being taken from the structural data, the mean plane of the real glass container shape is approximated by circles and straight lines. The angle between the tangents of adjacent segments at the point of contact is minimized and must be lower than 5°.

For the strength of a glass container the glass distribution is of significant importance. For this reason, the stress calculations are based on shapes and wall thickness data of sample bottles provided by two container ware producers.

The bottle outlines are transmitted onto paper by photoprinting. Following this the outlines are digi-

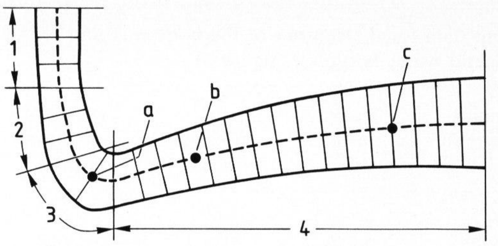

Figure 3. Element network of a part of the GDB-bottle bottom shape divided in regions 1, 2, 3, 4 with the nodes a, b, c.

tized. The deviation of the cutting plane from the mean plane and the distortion by the photoprint are considered. The outline data now have to be converted for further treatment. To describe the outer and inner contour a continuous curvature is produced by the splines. From these data the coordinates of the mean plane and the wall thickness at every point are calculated. This set of data is transformed to the representation by circles and straight lines as used in the finite element program.

The approximation of the actual bottle shape by circles and straight lines was difficult. The reason is not the limitation in the curvature shapes, but the large number of possible variations of the circles and line pieces. It was not possible to develop a converging approximation scheme in the given time. However, with a little more time spent very good approximations could be found.

3.2. Distribution of the element network

A further important criterion for the accuracy of the stress calculation is the number of elements which are generated to describe the object. The installed version of the finite element program can generate a maximum of 60 elements, so that for every given outline the stresses can be calculated at 121 nodes.

The following example shows how the element density influences the calculation result. For this purpose the outline has to be chosen small enough to enable a sufficient number of variations of the element density with respect to the given restrictions to be carried out. The bottom region is the most appropriate because it is small enough and regions with $R/w \approx 15$ and $R/w \approx 0.45$ are adjacent to each other. In this part of the bottle the highest stresses appear, so that it is of special importance to clarify the dependency of the calculated stresses on the element distribution.

The calculations are based on the part of a shape shown in figure 3. It is described by 4 regions which are divided in elements of approximately equal length. Table 1 shows the input data. All calculations were carried out with an internal pressure load of 2.75 MPa. With a constant number of elements in the

Table 1. Input data for the contour of the bottom region of the refillable mineral water bottle (cf. figure 3)

region	radius in mm	height in mm	wall thickness in mm	radius of curvature in mm
x	38.25	19.55	3.9	–
1	38.25	10.70	3.75	straight
2	36.85	4.85	4.8	straight
3	33.25	2.91	4.3	3.21
4	0	7.65	7.7	119

Table 2. Element distribution of the regions 1, 2 and 4 used in the test calculation (cf. figure 5)

calculation no.	region 1		region 2		region 4	
	n	l	n	l	n	l
1	3	2.95	2	3.01	11	3.06
2	4	2.21	3	2.01	16	2.11
3	6	1.48	4	1.50	23	1.47
4	8	1.11	5	1.20	29	1.16

Explanation: n = number of elements; l = element length.

regions 1, 2 and 4 and a varying number of elements in region 3, the stress distribution was calculated. For every element distribution the behavior of the wall stresses at three fixed points (cf. figure 3) has been observed. Figure 4 shows the internal longitudinal stresses as an example of the typical behavior of the calculated wall stresses. The calculated stresses are subject to considerable variations depending on the element distribution. With an increasing number of elements to describe the object, the calculated stresses approximate obviously to a limiting value.

It can also be seen that the stress behavior at the observed points in the neighboring, not varied regions is strongly coupled to the varied region. This dependency of single stresses on the stresses at more distant nodes is based on the fact that the entire nodes of the contour are coupled by the stiffness matrix. To eliminate this error a careful distribution of the finite elements at every part of the contour is necessary.

This behavior gives a reason for asking how quickly the influence between two regions will decrease with increasing distance. For this purpose the region 3 in figure 3 is resolved by 4 to 24 elements by steps of two. The resolution of the regions 1, 2 and 4 is shown in table 2. The wall stresses at different nodes of region 4 are taken and for all variations of the number of elements in region 3, the mean value and the standard deviation are calculated. Figures 5a and b show as an example the mean values of the internal longitudinal stresses in region 4 and the standard deviation as a function of the distance from the boundary between region 3 and region 4. A

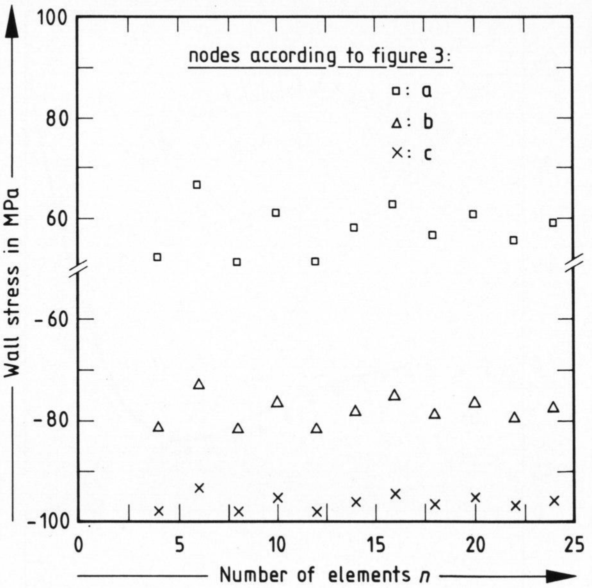

Figure 4. Variation behavior of the internal longitudinal stress at three nodes a, b, c depending on the number of elements in region 3 (cf. figure 3) of the bottom shape of the GDB-bottle.

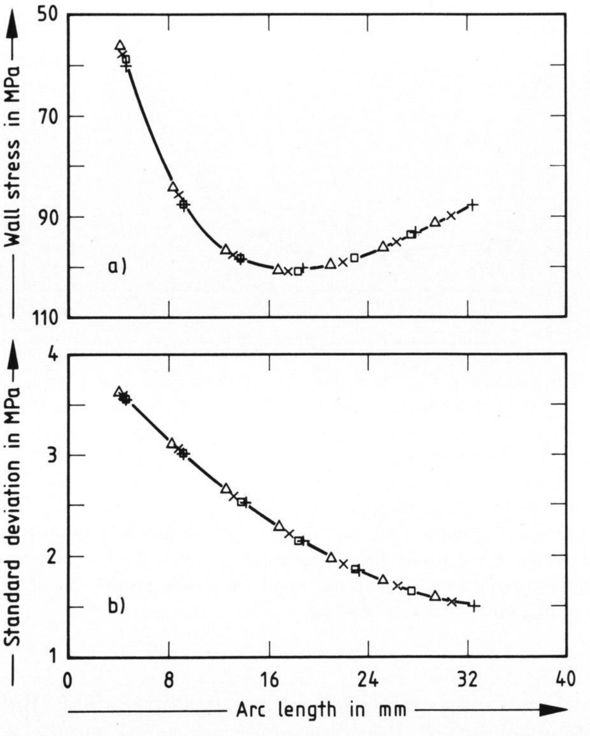

Figures 5a and b. Influence of the increasing distance from region 3 (cf. figure 3) on the development of a) the mean internal longitudinal stress, b) the standard deviation.
The average is taken from the values which result if the number of elements of region 3 is varied between 4 and 24 by steps of two, i.e. the values of figure 4.

dependency of the standard deviation on the mean wall stresses is not found. The standard deviation decreases with increasing distance to the varied region, the variation of the number of elements in the regions 1, 2 and 4 is without any influence.

While region 3 has a strong dependency of the stresses on the number of elements, in region 4 such a dependency is not detectable. The two regions differ through their very different curvature radii. Test calculations based on a hollow sphere show that these dependencies cannot be explained only by the radius of curvature or the radius of curvature to wall thickness ratio, but by the change of the radius of curvature to wall thickness ratio within a single element $\Delta(w/R)$. While the values of $\Delta(w/R)$ in region 4 lie between 0.0026 and 0.0001 for a single element, in region 3 values between 0.0389 and 0.0087 can be found. In figure 4 the stress for higher resolutions approaches a limiting value. From figure 4, a value for $\Delta(w/R)$ of about 0.005 per element can be estimated to be sufficiently accurate.

4. Applications of the finite element program

4.1. Calculation examples

In order to pay attention to the real glass distribution of glass containers, which is one of the most important properties with respect to the strength, half bottles were made available by two glass container producers (glassworks A and B). Specimen bottles from the same line had been subjected to a bursting pressure test. The data from this test were also made available. The outlines of the half bottles were treated as described in section 3.1. Based on the received sets of data stress calculations by the finite element program were carried out under the same load as the measured bursting pressure.

As mentioned in section 3.2., a maximum of 60 elements is possible. The real variations of wall thickness found in the half bottles are so great that the radius of curvature to wall thickness ratio of 0.005 per element, as demanded in section 3.2., cannot be held without a loss in resolution in other regions. For this reason $\Delta(w/R)$ is set to 0.02 per element.

The results of the stress calculations in the case of internal pressure loads are shown in figures 6a to f. The figures show circumferential stresses, i.e. in the direction of rotational symmetry, and longitudinal stresses, i.e. perpendicular to the rotational symme-

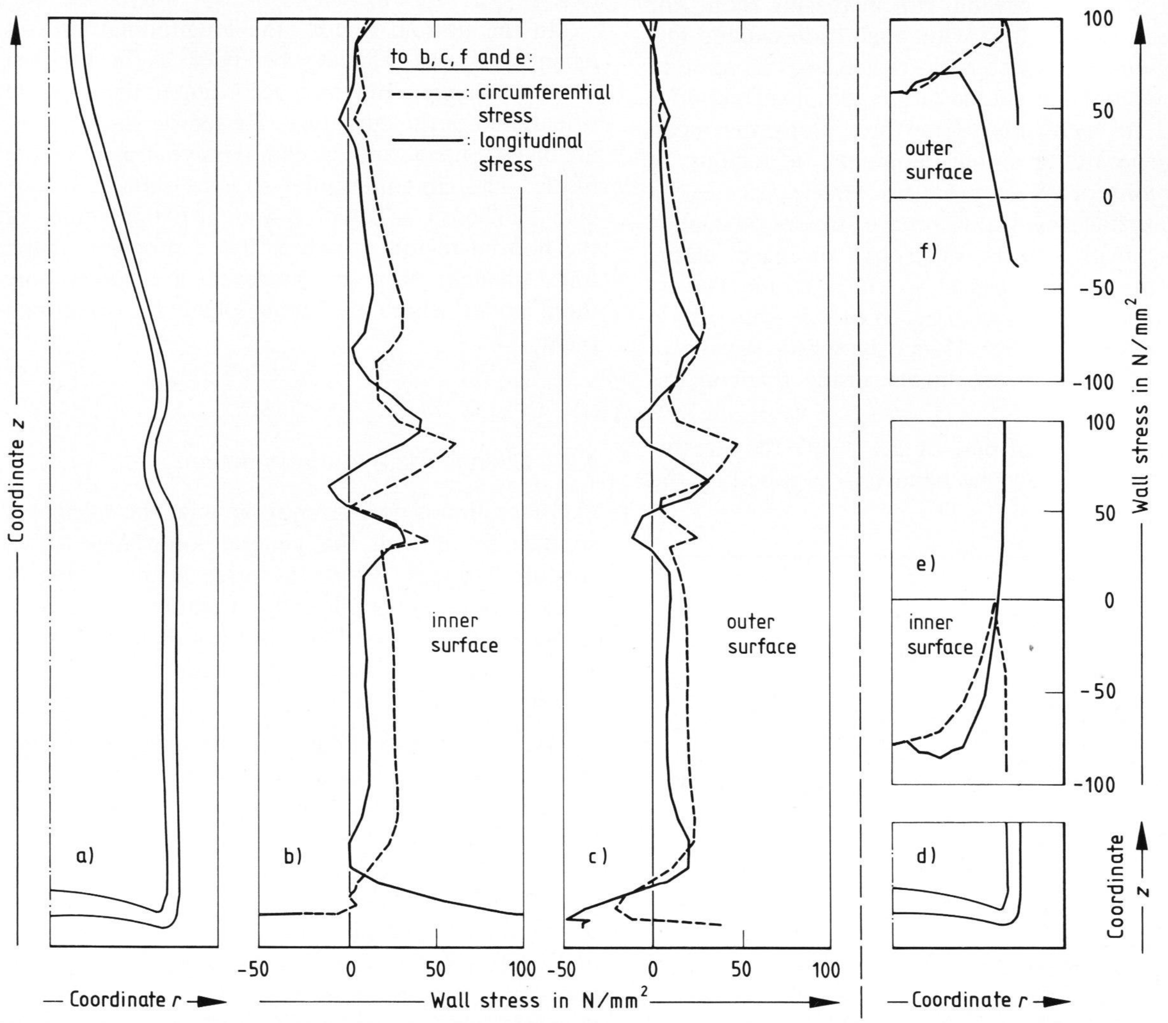

Figures 6a to f. Wall stress distributions of a GDB-bottle in the case of internal pressure load of 2.75 MPa; a) outline of the bottle, b) wall stress of the inner surface, c) wall stress of the outer surface, d) outline of the bottle bottom, e) wall stress of the inner surface of the bottle bottom, f) wall stress of the outer surface of the bottle bottom.

try and tangential to the contour. Positive values represent tensile stresses and negative values compressive stresses.

The stress distributions of the refillable mineral water bottle (GDB-bottle) in figures 6a to f show some characteristics of stress distributions in glass containers. Along the straight part between the mouth and the shoulder, in which the contour grows larger outwardly, the longitudinal and circumferential stresses both on the inner and outer surfaces grow with increasing radius. The circumferential stresses inside as well as outside are about 2.5 times higher than the longitudinal stresses. This behavior is according to the vessel formula.

Because of its design in the shoulder region, the GDB-bottle is a good example for demonstrating the dependency of the wall stresses on the bottle outline. In order to understand the resulting stresses one has to consider two forces: the planar force on the wall and a force along the mean plane, which is induced by the pressure against the lid and the bottom.

The planar force produces, according to the vessel formula, stresses growing with increasing radii. For the reason that regions with small radii expand less than regions with large radii, the stresses increase at small radii and decrease at large radii, if such regions are next to each other. The force along the mean plane generates bending moments in regions of curved contour. This produces tensile stresses on concave surfaces and compressive stresses on convex surfaces. Both effects superpose on each other. Outside the convex surfaces are of large radii, so that the influences work against each other; while inside both effects go together. Hence the tensile stresses in the shoulder region are higher inside than on the outside.

In the cylindrical part of the bottle the stresses follow approximately the behavior described by the vessel formula. The highest stresses appear at the strong curvature of the contour at the beginning of the bottom. In the course of the curve, the internal longitudinal stresses become very high, while the longitudinal stresses outside go through a considerable minimum. Large tensile stresses on the inside go together then with large compressive stresses on the outside. This behavior can again be explained by a bending moment induced by the neighboring regions. In the circumferential direction on the inner surface compressive stresses appear. These are characteristics which differ considerably from the results received by continuum model calculations. Probably, it is a property of the chosen element type, although, the circumferential stresses at this point of the contour are the only serious deviation from the expected stress behavior. The circumferential and the longitudinal stresses on the inner surface are known to be in the same range, so that an estimation of the appearing strain is still possible from the calculated longitudinal stresses. Outside, a tensile stress maximum is found for circumferential stress, which is of the same order as the longitudinal stress maximum inside.

In the bottom region, the longitudinal stresses again show the bending behavior as in the last described region; however, according to the opposite orientation of the curvature, the tensile stresses now are on the outside and the compressive stresses on the inside. The circumferential stresses show a similar course. There is a negative peak at the beginning of the bottom region, which is also a property of the finite element program; however, it involves only three nodes where the mean plane has a turning point.

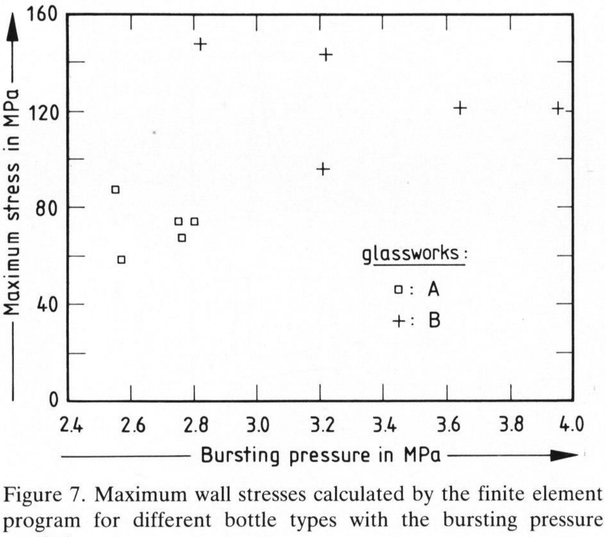

Figure 7. Maximum wall stresses calculated by the finite element program for different bottle types with the bursting pressure applied.

4.2. Strength data in the literature

Consideration is now given to how far the calculated stresses fit in with the general knowledge about fracture stresses. Over the past years, a lot of investigations concerning the fracture strength of glass have been carried out. Most of them have dealt with flat glass, because of the easier experimental conditions.

Detailed investigations into the strength of glass rods have been carried out by Varner and Oel [2]. For no-handled rods they found a mean fracture stress at the fracture origin of 80.4 MPa; for lightly damaged rods this value decreases to 55 MPa. Hence the strength of glass depends considerably on the state of the surface, which in turn depends on its treatment during production. From another source, container glass values of 28 to 62 MPa are achieved if blown in hot iron molds, 35 to 69 MPa if blown in paste molds and 104 to 280 MPa for the inner surface [6].

4.3. Maximum stress under internal pressure load

In order to test the bursting pressure, bottles of the two glassworks A and B were taken off the line directly after the annealing furnace. It can be assumed, as a very simple approximation that the distribution of flaws is the same all over the surface, if seeds or damage caused by production problems are excluded. In this case the container would fail at the point of maximum surface stress. The height of the critical stress must not depend on the shape and must also be independent of the bursting pressure. From the calculations in section 4.1., the maximum values of the longitudinal and circumferential stresses inside and outside are taken. In figure 7 the average maximum stresses of different shapes are shown. Each point characterises one bottle type. The values are subject to large variations, but a dependency on the shape or the bursting pressure cannot be found. Remarkable is the significant deviation of the maximum stresses between the two glassworks.

Possibly the parameters of the bursting pressure test differ in the two glassworks. Also differences concerning the handling of the bottles in the course of production are possible; however, these must be of fundamental nature, otherwise larger variations between different bottle types in the same glassworks would be detected. Except for one case, all maximum stresses lie in the region of the large curvature between the cylindrical part and the bottom of the bottle. In 10 cases the longitudinal stress inside reaches the highest value and in 15 cases the circumferential stress outside. The maximum stresses on the outer surface are clearly shifted in the direction of the cylindrical part of the contour, while the inside maximum stresses are found near the bottom region. In the case of the exception, a maximum circumferential stress lies inside the cylindrical part of the bottle.

The fracture stresses calculated with the finite element program are found to be in the same range as the fracture stresses stated in the literature, although the lower values found for one of the glassworks seem to fit better.

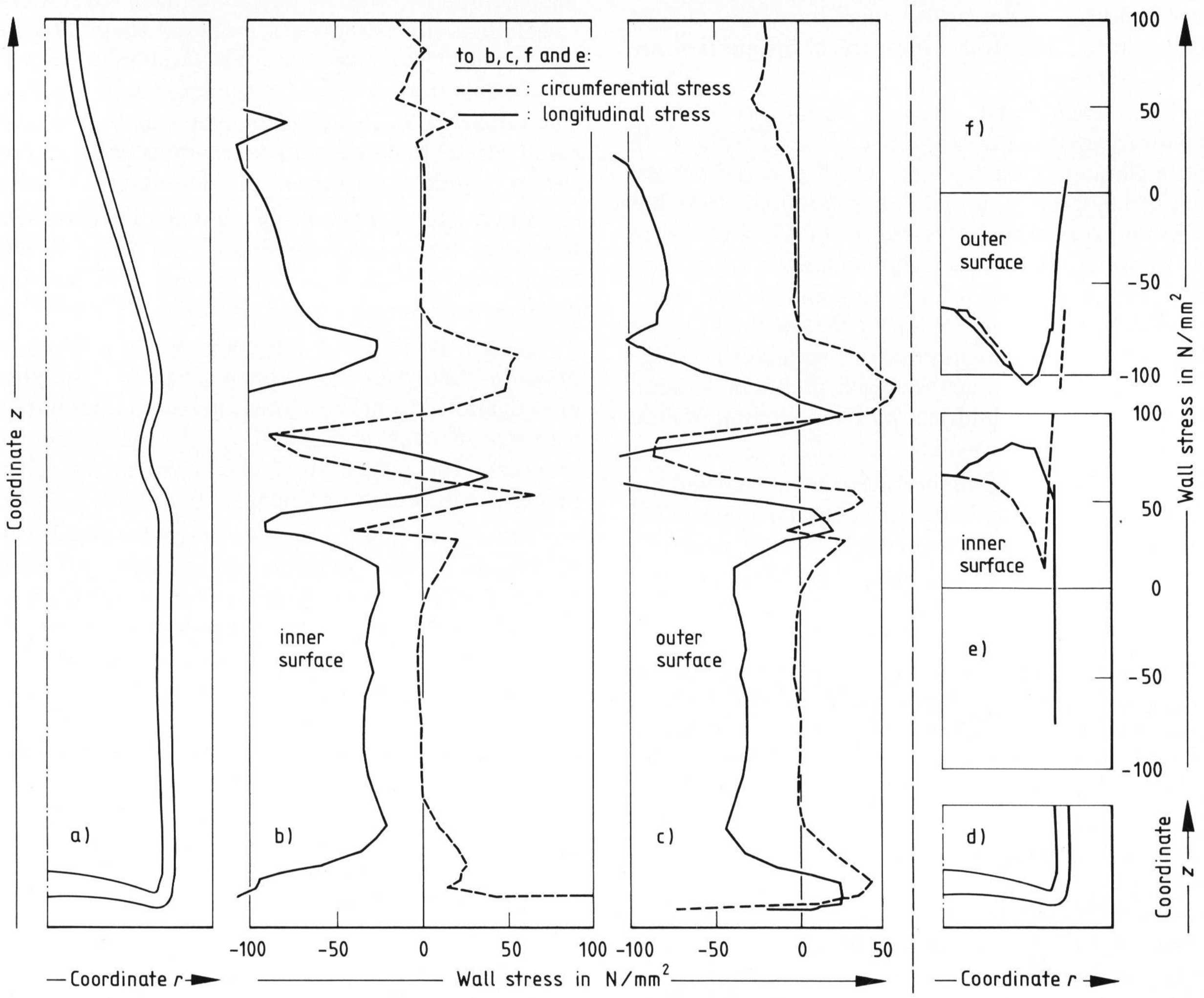

Figures 8a to f. Wall stress distributions of a GDB-bottle in the case of an axial load of 36 KN; a) outline of the bottle, b) wall stress of the inner surface, c) wall stress of the outer surface, d) outline of the bottle bottom, e) wall stress of the inner surface of the bottle bottom, f) wall stress of the outer surface of the bottle bottom.

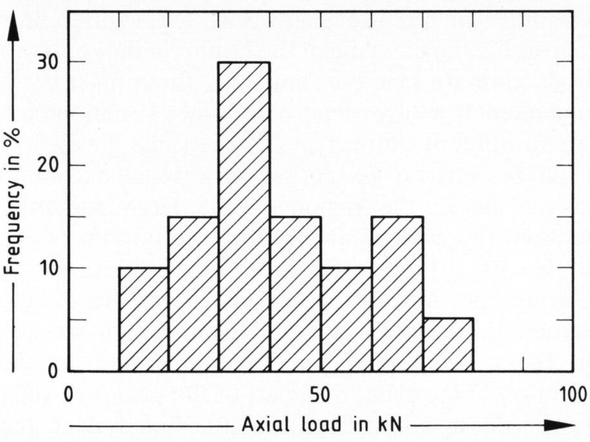

Figure 9. Distribution of the maximum axial load calculated by the finite element program for different bottle types. The calculations are based on the maximum stresses according to figure 7.

4.4. Maximum stresses under axial load

Beside the wall stress distributions in the case of internal pressure loading the finite element program can also calculate the stresses under axial load. Figures 8a to f show the corresponding stress distributions, again using the example of the GDB-bottle. The following typical properties are worth mentioning.

The longitudinal stresses, inside as well as outside, are compressive stresses from the mouth to the beginning of the bottom, which results from the type of load. The internal circumferential stress has its first maximum when the outline bends outwards to the shoulder. A further clear maximum in circumferential stress can be found inside and outside at the shoulder itself. In the region of the inclined part of the contour between mouth and shoulder, a force component becomes active which points in a radial direction. In the cylindrical part the circumferential stress drops to zero again.

At the contact region between the bottom and the cylindrical part of the bottle, the internal longitudinal stress remains compressive stress, while outside a tensile stress maximum appears. This maximum can be explained by the fact that the force points downwards through the bottle wall in the cylindrical part, but the support point is shifted slightly to the axis of the container. Here again a radial force is generated, which results in tensile stress maxima of the circumferential stress inside and outside. In the bottom region, the longitudinal and circumferential stresses inside become tensile stresses, the longitudinal and circumferential stresses outside become compressive stresses. This behavior can also be explained by the fact that the force through the cylindrical part does not point directly to the support point. The highest stresses under axial load appear in the bottom region between the container axis and the transition to the cylindrical part of the bottle. In only one case does the highest stress value lie in the shoulder region. 75 % of the calculated maximum stresses are internal longitudinal stresses, 10 % internal circumferential stresses and 15 % external circumferential stresses.

Axial load test data have not been available in this investigation; however, glassworks generally quote values between 30 and 50 kN. In order to likewise estimate, with respect to the axial load strength how well the calculation results and the state of knowledge fit, the axial load was determined at which the maximum stress of the bottles from glassworks A was 70 MPa and from glassworks B was 134 MPa. The resulting maximum axial loads are shown in figure 9. The values vary between 30 and 70 kN with a mean value of 45 kN. Hence the calculated maximum axial loads are in the same range as those found in practice.

5. Summary

A finite element program for calculating the wall stresses of container glass with respect to axial loads and internal pressure loads has been installed in a microcomputer with 64 kbyte storage. The stress calculations are based on a modified shell element which considers linear terms of the wall thickness/radius of curvature ratio and considers shearing forces. The efficiency of this element type was tested. The results of the finite element calculations and the consistent solutions found in the literature fit well.

The results of the finite element method generally depend on the element distribution. For this reason a criterion has been worked out by which an optimum element distribution can be chosen.

Sample bottles and the corresponding bursting pressure test data have been available for this investigation. From these data, maximum permitted wall stresses were calculated by the finite element program. The results are found to be in the same range as the literature values.

Thus, the finite element program enables a prediction of the influence of changes in glass container outline or in glass distribution quickly and with a sufficient degree of calculation accuracy.

*

These investigations were conducted with the kind support of the Arbeitsgemeinschaft Industrieller Forschungsvereinigungen e. V. (AIF), Köln, by agency of the Hüttentechnische Vereinigung der Deutschen Glasindustrie (HVG), Frankfurt am Main, through the resources of the Bundesministerium für Wirtschaft. Thanks are extended to the companies which provided the bottle outlines and the bursting pressure test data.

6. References

[1] Kerkhof, F.: Bruchmechanik von Glas und Keramik. T. 1//Grundlagen der Bruchmechanik. Sprechsaal **110** (1977) no. 7, p. 392–397.

[2] Varner, J. R.; Oel, H. J.: Einfluß von Oberflächenbeschädigungen auf die Festigkeit von Glasstäben. Glastech. Ber. **48** (1975) no. 5, p. 73–78.
[3] Sommer, E.: Bruchmechanische Bewertung von Oberflächenrissen. Berlin (et al.): Springer 1984.
[4] Kopetsch, H.: Erstellung eines Finite-Elemente-Programmes zur Festigkeitsanalyse axialsymmetrischer Behälter als Modul eines CAD-Systems zur Auslegung von Gußformen für die Glasflaschenfertigung. Rhein.-Westf. Tech. Hochschule Aachen, Dipl.-Arb. 1983.
[5] Timoshenko, S. P.; Woinowsky-Krieger, S.: Theory of plates and shells. 2nd ed. New York (et al.): McGraw-Hill 1959.
[6] Shand, E. B.: Glass engineering handbook. New York (et al.): McGraw-Hill 1958.

88R1393